Title

Magnitude-dependent and inversely-related osteogenic/chondrogenic differentiation of human mesenchymal stem cells under dynamic compressive strain

Journal

JOURNAL OF TISSUE ENGINEERING AND REGENERATIVE MEDICINE, 12(2)

ISSN

1932-6254

Authors

Horner, CB
Hirota, K
Liu, J
et al.

Publication Date

2018-02-01

DOI

10.1002/term.2455

Peer reviewed

Magnitude-Dependent and Inversely-related Osteogenic/Chondrogenic Differentiation of Human Mesenchymal Stem Cells by Dynamic Compressive Strain

Journal:	*Journal of Tissue Engineering and Regenerative Medicine*
Manuscript ID	TERM-16-0112.R1
Wiley - Manuscript type:	Research Article
Date Submitted by the Author:	n/a
Complete List of Authors:	Horner, Christopher; University of California, Bioengineering Hirota, Koji; University of California, Bioengineering Liu, Junze; University of California, Bioengineering Maldonado, Maricela; University of California, Bioengineering Park, Boris; University of California, Bioengineering Nam, Jin; University of California, Bioengineering
Keywords:	Human mesenchymal stem cell, Differentiation, Dynamic compression, Osteogenesis, Chondrogenesis, Electrospun scaffold

Magnitude-Dependent and Inversely-related Osteogenic/Chondrogenic Differentiation of Human Mesenchymal Stem Cells Under Dynamic Compressive Strain

Short title: Dynamic Compression Magnitude-dependent Differentiation of Human MSCs

Christopher B. Horner, Koji Hirota, Junze Liu, Maricela Maldonado, B. Hyle Park and Jin Nam*

Department of Bioengineering, University of California, Riverside, CA 92521

*corresponding author

Jin Nam, Ph.D.

Department of Bioengineering

University of California-Riverside

900 University Ave., Riverside, CA 92521

E-mail address: jnam@engr.ucr.edu

Phone: 951-827-2064

Abstract

Biomechanical forces have been shown to significantly affect tissue development, morphogenesis, pathogenesis and healing, especially in orthopaedic tissues. Such biological processes are critically related to the differentiation of human mesenchymal stem cells (hMSCs). However, the mechanistic details regarding how mechanical forces direct MSC differentiation and subsequent tissue formation are still elusive. Electrospun three-dimensional scaffolds were utilized to culture and subject hMSCs to various magnitudes of dynamic compressive strains at 5, 10, 15, or 20% ($\varepsilon = 0.05, 0.10, 0.15, 0.20$) at a frequency of 1 Hz for 2 hours daily for up to 28 days in osteogenic media. Gene expression of chondrogenic markers (*ACAN, COL2A1, SOX9*) and glycosaminoglycan (GAG) synthesis were upregulated in response to the increased magnitudes of compressive strain, whereas osteogenic markers (*COL1A1, SPARC, RUNX2*) and calcium deposition had noticeable decreases by compressive loading in a magnitude-dependent manner. Dynamic mechanical analysis showed enhanced viscoelastic modulus with respect to the increased dynamic strain peaking at 15%, which coincides with the maximal GAG synthesis. Furthermore, polarization-sensitive optical coherence tomography (PS-OCT) revealed that mechanical loading enhanced the alignment of extracellular matrix to the greatest level by 15% strain as well. Overall, we show that the degree of differentiation of hMSCs towards osteogenic or chondrogenic lineage is inversely related, and it depends on the magnitude of dynamic compressive strain. These results demonstrate that multi-phenotypic differentiation of hMSCs can be controlled by varying the strain regimens, providing a novel strategy to modulate differentiation specification and tissue morphogenesis.

Keywords: Human mesenchymal stem cell, Differentiation, Dynamic compression, Osteogenesis, Chondrogenesis, Electrospun scaffold

1. Introduction

Mesenchymal stems cells (MSCs) have shown a great potential as a cell source for the regeneration of diseased or damaged musculoskeletal tissues. They present capabilities to expand to a clinically relevant cell number and differentiate to multiple phenotypes for target tissues (Bianco *et al.*, 2001; Caplan and Dennis, 2006; Jiang *et al.*, 2002; Pittenger *et al.*, 1999). Furthermore, the use of autologous MSCs can also leverage their non-immunogenic or even immune-suppressive characteristics for enhanced host-tissue integration (Glowacki *et al.*, 2015; Griffin *et al.*, 2013; Nauta and Fibbe, 2007). For these reasons, there have been many clinical trials to utilize MSCs for tissue repair, typically by means of cell injection to the site of damage (Arthur *et al.*, 2009; Evans *et al.*, 2014; Jo *et al.*, 2014). Although some of the trials have shown excellent efficacies, the control of stem cell differentiation into a desired phenotype *in vivo* still presents a great challenge, especially in the mechanically challenging areas like cartilage defects (van Buul *et al.*, 2014; Wakitani *et al.*, 2004). In this regard, *in vitro* culture under well-defined physiochemical microenvironments of the cells via the use of a scaffold and/or a bioreactor provides an opportunity to precisely control stem cell behaviors (i.e., proliferation and differentiation of MSCs) for desired tissue formation prior to implantation.

Both biochemical and biophysical environments modulate cellular behaviors in skeletal tissues. Stimulating skeletal cells with biochemical factors utilizing growth factors and cytokines to initiate various signaling cascades has been the primary choice of directing tissue formation. Tissue growth factor beta (TGF-β) superfamily including TGF-β3, and BMP2 and BMP7 are well-known chondrogenic/osteogenic growth factors, and other small molecules including dexamethasone, ascorbic acid and beta-glycerophosphate have been shown to promote osteogenesis of MSCs (Boeuf and Richter, 2010; Goessler *et al.*, 2005; Langenbach and

Handschel, 2013; Shen *et al.*, 2010). However, mechanical stimulation has been also shown to be an essential component to functionalize and mature the tissues, especially in the musculoskeletal system (Candiani *et al.*, 2008; DuFort *et al.*, 2011; Jaalouk and Lammerding, 2009; Nam *et al.*, 2009; Nam *et al.*, 2013; Tonnarelli *et al.*, 2014). Indeed, a lack of mechanical stimulation during development results in malformation of bone and cartilage, substantiating its critical role in the regulation of skeletal tissue morphogenesis (Palomares *et al.*, 2009; Shea *et al.*, 2015). In many *in vitro* studies, both osteoblasts, the bone forming cell, and chondrocytes, the primary cell found in cartilage, are mechano-responsive regulating their metabolic activities under dynamic compressive loading (Mauck *et al.*, 2007; Mauck *et al.*, 2000; Roelofsen *et al.*, 1995). Interestingly, we have previously shown that such mechano-responsiveness of osteoblasts and chondrocytes is magnitude-dependent, each having an optimal level of mechanical stimulation that led to the maximal osteogenic and chondrogenic activities (Nam *et al.*, 2008; Rath *et al.*, 2008).

MSCs have also shown to be mechano-responsive as mechanical stimulation affects their phenotype specification. Specifically, dynamic compressive loading has been shown to induce the differentiation of MSCs towards osteoblastic or chondrocytic phenotypes (Huang *et al.*, 2010; Huang *et al.*, 2004; Michalopoulos *et al.*, 2012; Pelaez *et al.*, 2009). For example, MSCs cultured in partially demineralized bone scaffolds and subjected to mechanical loading exhibited significant increase in alkaline phosphatase and osteopontin transcription levels, demonstrating the osteogenicity of mechanical stimulation (Mauney *et al.*, 2004). Additionally, compressive loading has been shown to induce cartilaginous matrix formation from MSCs cultured in hyaluronan-gelatin composite scaffolds (Angele *et al.*, 2004). However, there is still a lack of comprehensive understanding in the phenotype specification of MSCs under simultaneous

biochemical and mechanical stimulation as most studies typically focus on analyzing the differentiation towards a single phenotype rather than holistically examining simultaneous multi-phenotypic differentiation. Indeed, Grayson et al. have shown that MSCs can simultaneously differentiate to a mixture of cell phenotypes including both osteoblast and chondrocyte (Grayson *et al.*, 2010). In addition, our previous studies showing the magnitude-dependency of cellular behaviors in skeletal cells under dynamic compressive loading suggest that the application regimen of mechanical stimulation may influence phenotype specification of MSCs (Nam *et al.*, 2008; Rath *et al.*, 2008). Therefore, it is important to comprehensively understand how biochemical and mechanical cues synergistically or antagonistically influence MSC differentiation and subsequent tissue formation, in order to achieve enhanced skeletal tissue morphogenesis.

In this study, we investigated the effects of mechanical stimulation in different magnitudes on MSC differentiation in the presence of biochemical cues. More specifically, human MSCs (hMSCs) were seeded into 3D electrospun scaffolds with appropriate mechanical resiliency for various magnitudes of long-term dynamic compression under a mild osteogenic biochemical condition. The differentiation of hMSCs and subsequent ECM maturation under different magnitudes of mechanical stimulation were mechanically, biochemically, and optically characterized in a comprehensive manner to determine phenotype specification of the cells and subsequent tissue morphogenesis. This work aims to provide an outlook on a chondro-inductive mechanical stimulus and its interaction with a mild osteogenic biochemical cue in a magnitude-dependent manner. Ultimately, these assessments will provide a clear insight to implement a certain regimen of dynamic mechanical stimulation to promote MSC differentiation towards a desired phenotype and tissue formation.

2. Materials and Methods

All reagents and products were purchased from Sigma–Aldrich (St. Louis, MO) unless otherwise noted.

2.1. Scaffold fabrication

Three-dimensional (3D) scaffolds were synthesized by electrospinning an 11 wt % poly(ε-caprolactone) (PCL) dissolved in 19:1 (v/v) chloroform-methanol solution. A vertical electrospinning setup was used with a tip-to-collector distance of 45 cm as previously described (Horner *et al.*, 2016). The polymer solution was dispensed at 11 mL/hr and the applied voltage was adjusted to approximately 16 kV to form a stable Taylor cone (Taylor, 1969). A 6 mm diameter biopsy punch (Integra Miltex, York, PA) was used to produce cylindrical scaffolds from as-spun fiber mats of approximately 3 mm-thickness. The cylindrical scaffolds were then plasma-treated at 30 W for 5 minutes, followed by collagen type I conjugation to improve cellular adhesion using a crosslinking agent, 100 mM N-hydroxysuccinimide (NHS)/N-(3-Dimethylaminopropyl)-N'-ethylcarbodiimide hydrochloride (EDAC) (Nam *et al.*, 2013). The scaffolds were sterilized by 70% ethanol for 12 hours followed by air dry. Sterilized scaffolds were stored at 4°C until cell seeding. The microstructure of the electrospun fibers was observed under a scanning electron microscope (SEM, TESCAN, Brno, Czech Republic), and the average fiber diameter was measured from of at least 50 fibers (n=50) using ImageJ software.

2.2. Cell culture

Human fetal bone marrow-derived mesenchymal stem cells (hMSCs) were purchased from Applied Biological Materials (Richmond, Canada) and were cultured until experimental use

between passages 7 and 10. The hMSCs were expanded with growth media (GM) composed of DMEM-F12 (Lonza, Anaheim, CA) supplemented with 15% FBS, 1% Penicillin-Streptomycin, and 100ng/mL bFGF in T75 flasks until they reached approximately 85-90% confluency. The scaffolds placed in a 24 well-plate were seeded with 60 µL of cell-suspended media at a concentration of approximately 33 million cells/mL. The capillary forces of the sterilized and dry 3D scaffolds allowed for complete cellular infiltration throughout the thickness of each scaffold. Confirmation of complete cellular infiltration was confirmed via nuclear staining of the vertical cross-section of the scaffold with 4',6-diamidino-2 phenylindole (DAPI, Vector Laboratories). The stained cross-section was imaged with an inverted microscope (Nikon Eclipse, Melville, NY) and several images were stitched together to show the entire thickness of the scaffold. The cell seeded scaffolds were incubated for 2 hours to induce cell attachment before filling with an additional 1 mL of GM. The cell/scaffold constructs were pre-cultured in GM for 5 days prior to being subjected to differentiation media and/or mechanical stimulation. The GM was exchanged to osteogenic differentiation media (OM) 24 hours prior to the application of mechanical stimulation. The OM was composed of low glucose DMEM supplemented with 10% FBS, 10 mM sodium-β-glycerophosphate, 200 µM ascorbic acid-2-phosphate, 100 nM dexamethasone, and 1% Penicillin-Streptomycin-Fungizone. This media composition induces weak osteogenic differentiation in 3D in the absence of vitamin D or BMP. The OM was exchanged at 50% volume every day, and a full volume exchange was conducted every fifth day. Except the duration of mechanical stimulation, the cell/scaffold constructs were placed onto an orbital shaker at 200 RPM to ensure complete media exchange throughout the entirety of the experiment.

2.3. Application of dynamic compressive strain and mechanical characterization of cell/scaffold constructs

A custom compression system modified from the previous report was utilized to apply various magnitudes of compressive strain to the cell/scaffold constructs (Nam *et al.*, 2008). Briefly, a nominal tare load of 0.02 N was used to ensure the scaffolds were in contact with the impermeable platens. Unconfined compression of the cell/scaffold constructs was conducted daily for 2 hours/day for up to 28 days of stimulation. Mechanical simulation was applied in four separate magnitudes of strain: 5, 10, 15, and 20% (i.e., ε = 0.05, 0.10, 0.15, and 0.20) of the scaffold thicknesses, where statically cultured samples (ε = 0%) serve as a control. During the mechanical stimulation, force responses were recorded from individual samples using load cells in the compression system, used for the calculation of mechanical properties. The elastic and viscoelastic mechanical properties were deconvoluted by analyzing the dynamic responses of the cell/scaffold constructs using the following equation adapted from a study (Vincent, 2012).

$$\sigma_0 = \varepsilon_0 E^* \sin(\omega t + \delta) \quad (1),$$

which can be further expanded to

$$\sigma_0 = \varepsilon_0 E' \sin(\omega t) + \varepsilon_0 E'' \cos(\omega t) \quad (2),$$

where σ_0 is the maximum stress, ε_0 is the maximum strain, ω is the compression frequency, δ is the phase delay between the force and displacement curves, E^* is the ratio of maximum stress to maximum strain, E' is the elastic modulus, and E'' is the viscoelastic modulus. Alternatively, control samples (ε = 0%) were cultured and subjected to a brief mechanical testing with ε = 10% at designated time points to assess the mechanical properties (n=6).

2.4. Gene expression analysis

Total RNA from the cell/scaffold constructs cultured for 14 or 28 days was extracted using an RNeasy Mini Kit (Qiagen, Valencia, CA), and cDNA synthesis was performed using iScript cDNA Synthesis Kit (Bio-Rad, Hercules, CA). Negative control samples were collected from cells cultured on tissue culture plastic without exposure to OM, 3D culture in the scaffold, or mechanical stimulation. Real-time PCR was performed to determine osteogenic and chondrogenic gene expression with various differentiation markers using the following custom primers: *GAPDH (forward) 5′*-GCAAATTCCATGGCACCGT-*3′ and (reverse) 5′*-TCGCCCCACTTGATTTTGG-*3′; COL1A1 (forward) 5′*-CAACCTGGATGCCATCAAAG-*3′ and (reverse) 5′*-TGCTGATGTACCAGTTCTTCTGG-*3’; SPARC (ON) (forward) 5′*-TGGACTCTGAGCTGACCGAATT-*3′ and (reverse) 5′*-AGAAGGTTGTTGTCCTCATCCC-*3′; RUNX2 (forward)5′*-GAATGCACTATCCAGCCACCTT-*3′ and (reverse) 5′*-TAGTGAGTGGTGGCGGACATAC-*3’; ACAN (forward) 5′*-GTGATCCTTACCGTAAAGCCCAT-*3′ and (reverse) 5′*-TCTCATTCTCAACCTCAGCGA-*3′; COL2A1 (forward) 5′*-GGCAATAGCAGGTTCACGTACA-*3′ and (reverse) 5′*-CGATAACAGTCTTGCCCCACTT-*3′; SOX9 (forward) 5′*-GAGGAAGTCGGTGAAGAACG-*3′ and (reverse) 5′*-ATCGAAGGTCTCGATGTTGG-*3′*. PCR data was analyzed by the comparative threshold cycle (C_T) method using *GAPDH* as an endogenous control (Livak and Schmittgen, 2001).

2.5. Morphological analysis by histology, scanning electron microscopy and optical coherence tomography

Histology was used to determine the protein expression from either osteogenic or chondrogenic phenotypes via alizarin red or alcian blue staining, respectively as previously

described (Nam *et al.*, 2013). Briefly, the scaffold sections were incubated in a 0.05% alizarin red or a 0.2% alcian blue solution before rinsing with DI water, mounted and observed under an inverted microscope.

To examine cell secreted extracellular matrix (ECM) by scanning electron microscopy (SEM), the cell/scaffold constructs were fixed in 10% formalin overnight, and sectioned horizontal to the height of the sample. The sections were then dehydrated as previously described (Nam *et al.*, 2007). Briefly, a sequential dehydration of 50%, 70%, 80%, 95%, and 100% ethanol, followed by 3:1, 1:1, and 1:3 Ethanol:Hexamethyldisilazane (HMDS, Ted Pella, Inc., Redding, CA) exchange was performed. Upon completion of drying the samples overnight, the sections were sputter-coated with platinum–palladium followed by imaging using an SEM.

The formalin-fixed samples were also imaged using a custom-built multi-functional spectral-domain optical coherence tomography system with a wavelength range centered in the 1300nm range (Wang *et al.*, 2012). Depth-resolved profiles of intensity and birefringence, with 512 points spanning 2.0mm, were acquired at a rate of 30Hz. Volumetric data sets composed of 200 frames with 2048 depth profiles each were acquired to span 1.5 x 1.5mm or 4 x 4mm lateral areas. Three-dimensional volumes of OCT intensity and cumulative phase retardation were used for structural imaging and quantification of the optical polarization properties of the samples.

2.6. Statistical analysis

All experiments were conducted with at least 4 samples (n = 4), and data is represented as mean ± standard deviation or standard error of means. Each set of data was subjected to analysis using SPSS (v.19.0) to determine statistical significance by one-way analysis of variance (ANOVA) with Tukey's HSD post-hoc. Alternatively, to correlate scaffold properties and

cellular behaviors as a response of mechanical stimulation, bivariate relationship was determined by Pearson's correlation. A value of $p \leq 0.05$ was regarded as statistically significant.

3. Results

3.1. Scaffold characterization

Mechanically resilient 3D electrospun microfibrous scaffolds were synthesized to investigate the effects of dynamic mechanical stimulation on the phenotype-specific differentiation of hMSCs. The scaffolds were composed of cylindrical fibers providing large pores for facile cellular infiltration upon cell seeding (**Figure 1A**). In addition, the microfiber possesses a porous surface morphology for enhanced cellular adhesion (**Figure 1B**). The average fiber diameter was 10.99 ± 0.42 μm (**Figure 1C**). The 3D scaffolds were cut from electrospun mats to have dimensions of 6 mm in diameter with an approximate thickness of 3 mm (**Figure 1D**). The average compressive modulus of the scaffolds was 32.5 ± 1.98 kPa. Cells penetrated throughout the entire thickness of the 3mm scaffolds as shown by the DAPI stained cross-section of cell seeded scaffolds (**Figure 1E**).

3.2. Cellular differentiation under static conditions

Human mesenchymal stem cells (hMSCs) were seeded into the scaffolds and statically cultured for up to 28 days in osteogenic media to determine the baseline differentiation behavior of the cells. The degree of differentiation towards osteogenic and chondrogenic lineages was determined by gene and protein expression (**Figure 2**). The gene expression of osteogenic markers *COL1A1, SPARC (ON) and RUNX2* were all upregulated proportionally to the culture duration in OM over the cells cultured on tissue culture plate (TCP) in GM. These results

positively correlate with the osteogenic ECM synthesis as evidenced by the calcium deposition within the cell/scaffold constructs (**Figure 2D**). In contrast, the same static culture conditions did not induce any significant degree of chondrogenesis as expected, evident by statistically insignificant regulation of chondrogenic markers including *ACAN, COL2A1* and *SOX9* (**Figure 2E-G**). The insignificant differentiation of hMSCs in the static conditions was confirmed by a low level of GAG staining, indicating that the cells preferentially differentiated towards the osteogenic lineage.

3.3. Dynamic mechanical analysis of cell/scaffold constructs

After establishing the baseline differentiation behaviors under the static condition, the cell/scaffold constructs were subjected to various magnitudes of dynamic compressive strain to elucidate the effects of mechanical stimulation on phenotype specific differentiation of hMSCs. During the course of 28 days of culture duration, the mechanical properties of the cell/scaffold constructs were simultaneously measured during dynamic mechanical stimulation (**Figure 3A**). The viscoelastic properties of the cell/scaffold constructs were revealed by the phase delay between the applied strain and the corresponding force under sinusoidal unconfined compression (**Figure 3B**). Given that the compression frequency of the scaffolds was maintained at 1 Hz for the different magnitudes of strain, the resulting strain rates varied depending on the magnitudes. Since the viscoelastic properties of the cell/scaffold constructs is strain rate-dependent, the overall mechanical responses were deconvoluted to elucidate elastic and viscoelastic moduli by using Equation (2) based on the observed phase delay (δ) (**Figure 3C**).

Figures 3D and **3E** show the evolution in the elastic and viscoelastic moduli of the cell/scaffold constructs, respectively, during the culture period of up to 28 days. At Day 0 of

culture immediately after cell seeding, the cell/scaffold constructs exhibited an elastic modulus of 30.43 ± 6.90 kPa, and a viscoelastic modulus of 4.09 ± 0.88 kPa (data not shown). There was no significant changes in the elastic modulus in all conditions after 7 days of mechanical stimulation with various magnitudes. The constructs that were not subjected to mechanical stimulation (0%) exhibited greater increases throughout the culture duration as compared to other conditions except the samples that were subjected to higher strain magnitudes (15% and 20%) at the later culture periods. In contrast, the viscoelastic moduli of the constructs that were subjected to dynamic strains greater than 10% exhibited significant increases over the statically cultured constructs. In general, both elastic and viscoelastic moduli increased over the course of culture duration regardless of mechanical stimulation conditions. More importantly, the 15% strain condition induced the greatest increase in viscoelastic modulus as well as elastic modulus at 20.59 ± 4.67 kPa and 145.42 ± 24.64 kPa, respectively, suggesting the most significant ECM deposition over other conditions.

3.4. Magnitude-dependent osteogenic/chondrogenic differentiation of hMSCs under mechanical stimulation

To determine the effects of mechanical stimulation at the transcriptional level that modulated the differentiation of hMSCs, the expression of osteogenic or chondrogenic genes were examined. These genes are known to regulate phenotype-specific ECM deposition, which likely affected the evolution of mechanical properties. As previously noted in **Figure 2**, the static culture condition ($\varepsilon = 0\%$) in osteogenic media induced gradual osteogenesis, indicated by increases in all osteogenic markers *COL1A1, SPARC (ON) and RUNX2* over the course of 28 days (**Figure 4A-C**). Interestingly, the application of dynamic compression suppressed many of

these osteogenic markers except *RUNX2* which had a significantly greater expression in the 20% strain condition as compared to the statically cultured condition at Day 28.

Unlike osteogenesis, dynamic compressive strains enhanced the chondrogenesis of hMSCs cultured in the 3D scaffolds in general (**Figure 4D-F**). Both *COL2A1* and *SOX9* exhibited upregulation by mechanical stimulation in the most conditions while *ACAN* showed the greatest expression at the 15% strain. As expected, the expression pattern of chondrogenic genes were closely related to the mechanical properties of the cell/scaffold constructs, especially viscoelastic properties: both showed the maximums when dynamic compressive strain of 15% was applied during the culture.

3.5. Magnitude-dependent ECM deposition/alignment by dynamic mechanical stimulation

In order to assess tissue maturation, ECM deposition was examined by SEM and histology at the culture durations of 14 and 28 days for the cell/scaffold constructs that were either subjected (ε = 5, 10, 15 & 20%) or not subjected (ε = 0%) to dynamic compression (**Figure 5**). The horizontal sections of both the top and the middle were observed to determine the uniformity of cellular growth/ECM secretion. In all cases, the pores within the scaffolds were densely populated by cell-secreted ECMs as early as the culture duration of 14 days. These ECMs were further specified by histological examination with osteogenic and chondrogenic-specific stains, i.e., alizarin red for calcium deposition and alcian blue for GAG, respectively (**Figure 6**). For alizarin red staining, the static culture condition showed the greatest calcium deposition, which gradually decreased with increasing the magnitude of dynamic compressive strain for both 14 and 28 days of culture. In contrast, GAG deposition determined by alcian blue

staining was gradually enhanced with the increased magnitude of dynamic compression, peaking at 15% strain, followed by a slight decrease at 20% strain.

The morphological changes of the cell/scaffold constructs after 28 days of culture under various magnitudes of dynamic compression were further examined by OCT (**Figure 7**). Differences between the samples can be seen in 3D reconstructed volumes of the samples (**Figure 7A**, Supplementary Data). The cylindrical structure of the fibers that is very clearly evident in the absence of cells becomes obscured in the sample seeded with cells under no compression, and becomes visible under compression. Interestingly, polarization-sensitive OCT (PS-OCT) reveals more quantifiable differences between the samples that relate to their differences in ECM organization (**Figure 7B**). Quantitative analysis of the cumulative phase retardation as a function of depth was done for cell/scaffold constructs of all conditions as compared to acellular scaffolds. PS-OCT detects form birefringence, which is proportional to the density and organization of fibrous structures and can be quantified through determination of the rate at which the cumulative phase retardation between orthogonal polarization states changes with depth in a sample. The alignment of deposited ECM, characterized by the initial offset and the slope of depth-dependent phase retardation, was closely related to the magnitude of applied strains during culture; 0% exhibited the most random ECM orientation, evident by a uniform low phase retardation before an increase due to signal weakening. In contrast, the cell/scaffold constructs subjected to dynamic compression during culture exhibited greater intensities and rapid increases in phase retardation, suggesting alignment of ECMs as compared to the statically cultured constructs. Among the dynamic culture conditions, 15% strain induced the greatest alignment of the ECM, coinciding with the observed greatest elastic and viscoelastic moduli.

4. Discussion

Biomechanical factors continuously modulate tissue morphogenesis throughout development, especially in the musculoskeletal system. It has been shown that limited mechanical loading (e.g., immobilization or disuse) during development prevents or retards musculoskeletal tissue morphogenesis (Shea *et al.*, 2015), suggesting the critical role of mechanical stimulation in tissue specification including stem cell differentiation and maturation. In this regard, many studies have utilized dynamic mechanical stimulation in a variety of forms such as compression, tension and shear, as a biological cue to enhance tissue morphogenesis for bone and cartilage from MSCs (Delaine-Smith and Reilly, 2011; Huang *et al.*, 2004; Jagodzinski *et al.*, 2008; Kreke *et al.*, 2008). Although those exploratory studies clearly demonstrated the anabolic effects of mechanical stimulation, they were typically focused on the differentiation of MSCs towards a single phenotype without a comprehensive understanding in the multi-phenotypic differentiation of the cells under the synergistic and antagonistic effects of biochemical cues and dynamic mechanical stimulation. With the end goal of producing physiologically relevant tissue constructs which can ultimately be used as *in vitro* tissue models or replacements for diseased or damaged skeletal tissues, we present here the fundamental aspects of mechano-modulation in hMSC differentiation and maturation. Specifically, our systematic approach revealed that dynamic compressive strain suppresses biochemically directed osteogenesis while promoting chondrogenesis of hMSCs in a magnitude-dependent manner.

Both biochemical and biophysical factors modulate stem cell differentiation (Howard *et al.*, 2011). When hMSCs were seeded into the scaffold and subjected to osteogenic media, they preferentially differentiated towards osteoblasts as expected. Interestingly, when the cell/scaffold constructs were subjected to dynamic compression in the same osteogenic media, however, the

cells concurrently differentiated towards both osteoblasts and chondrocytes. This strongly suggests the critical role of biomechanical factors determining cellular fate, even overcoming local biochemical environments. More significantly, such mechano-responsiveness is magnitude- and phenotype-specific. The cells not subjected to mechanical loading exhibited mostly osteoblastic traits, whereas those exposed to dynamic compression decreased the degree of osteogenic differentiation, inversely proportional to the magnitude of strain applied. This cellular response conflicts with the previous report, where the dynamic compression enhanced the anabolic activities of mature osteoblasts (Rath *et al.*, 2008), likely demonstrating phenotype-specific actions of mechanical stimulation. Conversely, the degree of chondrogenic differentiation was positively correlated to the magnitude of dynamic compression, peaking at 15% strain. Interestingly, there was a decrease in the chondrogenic expression for gene and protein expression, as well as mechanical properties, in the 20% applied strain condition, which is in agreement with previously established findings where over-stimulation of MSCs can be detrimental to chondrogenesis (Elder *et al.*, 2001). The upregulation of *RUNX2* may be due to over-loading induced inflammation, but requires further investigation to determine the mechanistic details. These results suggest that over-stimulation of the cell/scaffold constructs beyond a specific threshold may actually be detrimental to mature tissue development.

In addition to phenotype specification of hMSCs, mechanical stimulation strongly affected ECM production and organization. Evident from histological imaging, the magnitude of dynamic compressive strain differentially regulated phenotype-specific ECM production. Greater amount of mineral deposition at lower magnitudes was observed while higher magnitudes enhanced GAG production. This observation is well aligned with the mechanical characterization of the cell/scaffold constructs, where viscoelastic modulus was clearly correlated to the intensity

of GAG stains in **Figure 6**. In addition to ECM production, mechanical stimulation also modulated the organization of ECM. PS-OCT was utilized, for the first time in engineered tissues at the best of our knowledge, to determine dynamic strain magnitude-dependent ECM alignment. Indeed, the cell/scaffold constructs subjected to 15% strain showed the greatest ECM alignment, demonstrating the capability of mechanical stimulation to organize ECMs as often observed *in vivo* in cartilage and bone (Sharma and Elisseeff, 2004). The direction of the alignment with respect to the depth of the cell/scaffold constructs was not investigated in this study. Nevertheless, these results suggests a great potential of dynamic compressive loading to mimic the organized structure of cartilage ECMs.

The comprehensive analysis of the biochemical and mechanical properties of the dynamically cultured scaffolds provides insight into how various magnitudes of strain differentially influence musculoskeletal tissue development. Our results indicate that stem cell differentiation is dynamic strain magnitude-dependent in the presence of a biochemical cue. These results provide a greater understanding in how mechanical cues may override the directed biochemical cues to provide a foundation for tissue engineering. This may address the challenges to form neo-tissue composed of multi-cell types, by regulating the combination of local biochemical and mechanical factors in a spatially controlled manner; we are currently investigating simultaneous differentiation of MSCs towards osteoblasts and chondrocytes to form osteochondral tissues within a monolithic scaffold with heterogeneous mechanical properties. Our study therefore suggests a new outlook on directing MSC differentiation towards musculoskeletal tissues by utilizing the mutual effects of biochemical and magnitude-dependent mechanical cues.

5. Conclusion

Mechanical stimulation provides a facile means to direct stem cell differentiation in lieu of biochemical cues. In this study, we demonstrated that MSCs differentiate in a magnitude-dependent and phenotype-specific manner in response to different magnitudes of applied dynamic compressive strain. Ultimately, these results suggest that MSCs are mechano-responsive and their multi-phenotypic differentiation can be controlled by varying the strain regimens. The results, therefore, provide a novel strategy to modulate phenotype-specific MSC differentiation and subsequent tissue morphogenesis.

6. Acknowledgments

This work was supported by UCR initial complement funding and through the CAL_BRAIN program (349329).

References

Angele P, Schumann D, Angele M, Kinner B, Englert C, Hente R, Fuchtmeier B, Nerlich M, Neumann C, Kujat R. 2004, Cyclic, mechanical compression enhances chondrogenesis of mesenchymal progenitor cells in tissue engineering scaffolds, *Biorheology*, **41**: 335-346

Arthur A, Zannettino A, Gronthos S. 2009, The therapeutic applications of multipotential mesenchymal/stromal stem cells in skeletal tissue repair, *Journal of cellular physiology*, **218**: 237-245

Bianco P, Riminucci M, Gronthos S, Robey PG. 2001, Bone marrow stromal stem cells: nature, biology, and potential applications, *Stem cells*, **19**: 180-192

Boeuf S, Richter W. 2010, Chondrogenesis of mesenchymal stem cells: role of tissue source and inducing factors, *Stem Cell Res Ther*, **1**: 31

Candiani G, Raimondi MT, Aurora R, Lagana K, Dubini G. 2008, Chondrocyte response to high regimens of cyclic hydrostatic pressure in 3-dimensional engineered constructs, *Int J Artif Organs*, **31**: 490-499

Caplan AI, Dennis JE. 2006, Mesenchymal stem cells as trophic mediators, *Journal of cellular biochemistry*, **98**: 1076-1084

Delaine-Smith RM, Reilly GC. 2011, The effects of mechanical loading on mesenchymal stem cell differentiation and matrix production, *Vitamins and hormones*, **87**: 417-480

DuFort CC, Paszek MJ, Weaver VM. 2011, Balancing forces: architectural control of mechanotransduction, *Nature reviews. Molecular cell biology*, **12**: 308-319

Elder SH, Goldstein SA, Kimura JH, Soslowsky LJ, Spengler DM. 2001, Chondrocyte differentiation is modulated by frequency and duration of cyclic compressive loading, *Annals of biomedical engineering*, **29**: 476-482

Evans CH, Kraus VB, Setton LA. 2014, Progress in intra-articular therapy, *Nature reviews. Rheumatology*, **10**: 11-22

Glowacki AJ, Gottardi R, Yoshizawa S, Cavalla F, Garlet GP, Sfeir C, Little SR. 2015, Strategies to direct the enrichment, expansion, and recruitment of regulatory cells for the treatment of disease, *Annals of biomedical engineering*, **43**: 593-602

Goessler UR, Bugert P, Bieback K, Deml M, Sadick H, Hormann K, Riedel F. 2005, In-vitro analysis of the expression of TGFbeta -superfamily-members during chondrogenic differentiation of mesenchymal stem cells and chondrocytes during dedifferentiation in cell culture, *Cell Mol Biol Lett*, **10**: 345-362

Grayson WL, Bhumiratana S, Grace Chao PH, Hung CT, Vunjak-Novakovic G. 2010, Spatial regulation of human mesenchymal stem cell differentiation in engineered osteochondral constructs: effects of pre-differentiation, soluble factors and medium perfusion, *Osteoarthritis and cartilage / OARS, Osteoarthritis Research Society*, **18**: 714-723

Griffin MD, Ryan AE, Alagesan S, Lohan P, Treacy O, Ritter T. 2013, Anti-donor immune responses elicited by allogeneic mesenchymal stem cells: what have we learned so far?, *Immunol Cell Biol*, **91**: 40-51

Horner CB, Ico G, Johnson J, Zhao Y, Nam J. 2016, Microstructure-dependent mechanical properties of electrospun core-shell scaffolds at multi-scale levels, *Journal of the mechanical behavior of biomedical materials*, **59**: 207-219

Howard J, Grill SW, Bois JS. 2011, Turing's next steps: the mechanochemical basis of morphogenesis, *Nature reviews. Molecular cell biology*, **12**: 392-398

Huang AH, Farrell MJ, Kim M, Mauck RL. 2010, Long-Term Dynamic Loading Improves the Mechanical Properties of Chondrogenic Mesenchymal Stem Cell-Laden Hydrogels, *Eur Cells Mater*, **19**: 72-85

Huang CY, Hagar KL, Frost LE, Sun Y, Cheung HS. 2004, Effects of cyclic compressive loading on chondrogenesis of rabbit bone-marrow derived mesenchymal stem cells, *Stem cells*, **22**: 313-323

Jaalouk DE, Lammerding J. 2009, Mechanotransduction gone awry, *Nature reviews. Molecular cell biology*, **10**: 63-73

Jagodzinski M, Breitbart A, Wehmeier M, Hesse E, Haasper C, Krettek C, Zeichen J, Hankemeier S. 2008, Influence of perfusion and cyclic compression on proliferation and differentiation of bone marrow stromal cells in 3-dimensional culture, *Journal of biomechanics*, **41**: 1885-1891

Jiang Y, Jahagirdar BN, Reinhardt RL, Schwartz RE, Keene CD, Ortiz-Gonzalez XR, Reyes M, Lenvik T, Lund T, Blackstad M, Du J, Aldrich S, Lisberg A, Low WC, Largaespada DA, Verfaillie CM. 2002, Pluripotency of mesenchymal stem cells derived from adult marrow, *Nature*, **418**: 41-49

Jo CH, Lee YG, Shin WH, Kim H, Chai JW, Jeong EC, Kim JE, Shim H, Shin JS, Shin IS, Ra JC, Oh S, Yoon KS. 2014, Intra-articular injection of mesenchymal stem cells for the treatment of osteoarthritis of the knee: a proof-of-concept clinical trial, *Stem cells*, **32**: 1254-1266

Kreke MR, Sharp LA, Lee YW, Goldstein AS. 2008, Effect of intermittent shear stress on mechanotransductive signaling and osteoblastic differentiation of bone marrow stromal cells, *Tissue engineering. Part A*, **14**: 529-537

Langenbach F, Handschel J. 2013, Effects of dexamethasone, ascorbic acid and beta-glycerophosphate on the osteogenic differentiation of stem cells in vitro, *Stem Cell Res Ther*, **4**: 117

Livak KJ, Schmittgen TD. 2001, Analysis of relative gene expression data using real-time quantitative PCR and the 2− ΔΔCT method, *methods*, **25**: 402-408

Mauck RL, Byers BA, Yuan X, Tuan RS. 2007, Regulation of cartilaginous ECM gene transcription by chondrocytes and MSCs in 3D culture in response to dynamic loading, *Biomechanics and modeling in mechanobiology*, **6**: 113-125

Mauck RL, Soltz MA, Wang CCB, Wong DD, Chao PHG, Valhmu WB, Hung CT, Ateshian GA. 2000, Functional tissue engineering of articular cartilage through dynamic loading of chondrocyte-seeded agarose gels, *J Biomech Eng-T Asme*, **122**: 252-260

Mauney JR, Sjostorm S, Blumberg J, Horan R, O'Leary JP, Vunjak-Novakovic G, Volloch V, Kaplan DL. 2004, Mechanical stimulation promotes osteogenic differentiation of human bone marrow stromal cells on 3-D partially demineralized bone scaffolds in vitro, *Calcified tissue international*, **74**: 458-468

Michalopoulos E, Knight RL, Korossis S, Kearney JN, Fisher J, Ingham E. 2012, Development of methods for studying the differentiation of human mesenchymal stem cells under cyclic compressive strain, *Tissue engineering. Part C, Methods*, **18**: 252-262

Nam J, Aguda BD, Rath B, Agarwal S. 2009, Biomechanical thresholds regulate inflammation through the NF-κB pathway: experiments and modeling, *PLoS One*, **4**: e5262

Nam J, Huang Y, Agarwal S, Lannutti J. 2007, Improved cellular infiltration in electrospun fiber via engineered porosity, *Tissue engineering*, **13**: 2249-2257

Nam J, Perera P, Rath B, Agarwal S. 2013, Dynamic regulation of bone morphogenetic proteins in engineered osteochondral constructs by biomechanical stimulation, *Tissue engineering. Part A*, **19**: 783-792

Nam J, Rath B, Knobloch TJ, Lannutti JJ, Agarwal S. 2008, Novel electrospun scaffolds for the molecular analysis of chondrocytes under dynamic compression, *Tissue engineering. Part A*, **15**: 513-523

Nauta AJ, Fibbe WE. 2007, Immunomodulatory properties of mesenchymal stromal cells, *Blood*, **110**: 3499-3506

Palomares KT, Gleason RE, Mason ZD, Cullinane DM, Einhorn TA, Gerstenfeld LC, Morgan EF. 2009, Mechanical stimulation alters tissue differentiation and molecular expression during bone healing, *J Orthop Res*, **27**: 1123-1132

Pelaez D, Huang CY, Cheung HS. 2009, Cyclic compression maintains viability and induces chondrogenesis of human mesenchymal stem cells in fibrin gel scaffolds, *Stem cells and development*, **18**: 93-102

Pittenger MF, Mackay AM, Beck SC, Jaiswal RK, Douglas R, Mosca JD, Moorman MA, Simonetti DW, Craig S, Marshak DR. 1999, Multilineage potential of adult human mesenchymal stem cells, *Science*, **284**: 143-147

Rath B, Nam J, Knobloch TJ, Lannutti JJ, Agarwal S. 2008, Compressive forces induce osteogenic gene expression in calvarial osteoblasts, *Journal of biomechanics*, **41**: 1095-1103

Roelofsen J, Klein-Nulend J, Burger EH. 1995, Mechanical stimulation by intermittent hydrostatic compression promotes bone-specific gene expression in vitro, *Journal of biomechanics*, **28**: 1493-1503

Sharma B, Elisseeff JH. 2004, Engineering structurally organized cartilage and bone tissues, *Annals of biomedical engineering*, **32**: 148-159

Shea CA, Rolfe RA, Murphy P. 2015, The importance of foetal movement for co-ordinated cartilage and bone development in utero : clinical consequences and potential for therapy, *Bone & joint research*, **4**: 105-116

Shen B, Wei A, Whittaker S, Williams LA, Tao H, Ma DD, Diwan AD. 2010, The role of BMP-7 in chondrogenic and osteogenic differentiation of human bone marrow multipotent mesenchymal stromal cells in vitro, *J Cell Biochem*, **109**: 406-416

Taylor G, 1969. Electrically driven jets, Proceedings of the Royal Society of London A: Mathematical, Physical and Engineering Sciences. The Royal Society, pp. 453-475.

Tonnarelli B, Centola M, Barbero A, Zeller R, Martin I. 2014, Re-engineering development to instruct tissue regeneration, *Current topics in developmental biology*, **108**: 319-338

van Buul GM, Siebelt M, Leijs MJ, Bos PK, Waarsing JH, Kops N, Weinans H, Verhaar JA, Bernsen MR, van Osch GJ. 2014, Mesenchymal stem cells reduce pain but not degenerative changes in a mono-iodoacetate rat model of osteoarthritis, *J Orthop Res*, **32**: 1167-1174

Vincent J, 2012. Structural biomaterials. Princeton University Press, Princeton, NJ, USA.

Wakitani S, Mitsuoka T, Nakamura N, Toritsuka Y, Nakamura Y, Horibe S. 2004, Autologous bone marrow stromal cell transplantation for repair of full-thickness articular cartilage defects in human patellae: two case reports, *Cell transplantation*, **13**: 595-600

Wang Y, Oh CM, Oliveira MC, Islam MS, Ortega A, Park BH. 2012, GPU accelerated real-time multi-functional spectral-domain optical coherence tomography system at 1300nm, *Opt Express*, **20**: 14797-14813

Figure Legends

Figure 1. **Morphological characterization of electrospun scaffolds.** Representative SEM images showing (**A**) the microstructure of the fibrous network of fibers having (**B**) the porous surface morphology and (**C**) a relatively uniform fiber size distribution (n=50). (**D**) A representative optical image showing the gross morphology and shape of the scaffolds for cell culture as well as (**E**) a DAPI stained image of a scaffold cross-section depicting complete cellular infiltration throughout the scaffold.

Figure 2. **The osteogenic or chondrogenic differentiation of hMSCs cultured in 3D electrospun scaffolds for various durations.** (**A-C**) Greater osteogenic gene expression (*COL1A1, SPARC (ON),* and *RUNX2*) and (**D**) ECM deposition (calcium by alizarin red) as compared to (**E-G**) chondrogenic gene expression (*ACAN, COL2A2,* and *SOX9*) and (**H**) ECM deposition (glycosaminoglycan by alcian blue) indicate preferential differentiation of hMSCs towards osteogenic lineage under static culture conditions.

Figure 3. Dynamic mechanical analysis of cell/scaffold constructs cultured under daily mechanical stimulation with various dynamic compressive magnitudes and culture durations. (**A**) A representative force and position curves acquired from a cell/scaffold construct under sinusoidal dynamic compression, and (**B**) a detailed force-position curves showing a phase delay (δ) between the applied strain and the responding force, which was used to deconvolute (**C**) the of elastic (*E'*) and viscoelastic (*E"*) moduli. **(D)** Deconvoluted elastic and (**E**) viscoelastic mechanical properties of the cell/scaffold constructs cultured under different

magnitudes (5, 10, 15 and 20% strain) of dynamic compression analyzed at different time points up to 28 days. * and ** denote $p < 0.05$ and $p < 0.01$, respectively (n=6).

Figure 4. **The osteogenic or chondrogenic differentiation of hMSCs by dynamic compressive stimulation with various magnitudes and durations.** The relative gene expression of hMSCs dynamically cultured in electrospun scaffolds for up to 28 days determined by qRT-PCR for (**A-C**) osteogenic markers, *COL1A1, SPARC (ON) and RUNX2*, and (**D-F**) chondrogenic markers *ACAN, COL2A1* and *SOX9*. Each gene expression was normalized to that of the cells before being cultured in the scaffold (dashed lines). * and ** denote $p < 0.05$ and $p < 0.01$, respectively, as compared to the negative control samples (represented as dashed lines); § and §§ denote $p < 0.05$ and 0.01, respectively, as compared statically culture samples (0%).

Figure 5. **Representative SEM images of cell/scaffold constructs cultured under various conditions.** The cell/scaffold constructs cultured under different dynamic compressive stimulation (0, 5, 10, 15 and 20% strain) for 14 or 28 days were subjected to SEM imaging to assess overall ECM deposition.

Figure 6. **Representative histology images of cell/scaffold constructs cultured under various conditions exhibiting different ECM compositions from hMSCs.** The cell/scaffold constructs cultured under different dynamic compressive stimulation (0, 5, 10, 15 and 20% strain) for 14 or 28 days were subjected to histology imaging (alizarin red for calcium and alcian blue for glycosaminoglycan) to assess overall ECM deposition. A macro-scale digital image of scaffold sections at day 28 is also shown.

Figure 7. Optical Coherence Tomography (OCT) of acellular and cellular scaffolds cultured with or without dynamic compression. OCT intensity images of (**A**) acellular scaffold, cell/scaffold constructs cultured (**B**) without or (**C**) with dynamic compression, and (**D-F**) corresponding graphs of double-pass cumulative birefringence from polarization-sensitive OCT analysis.

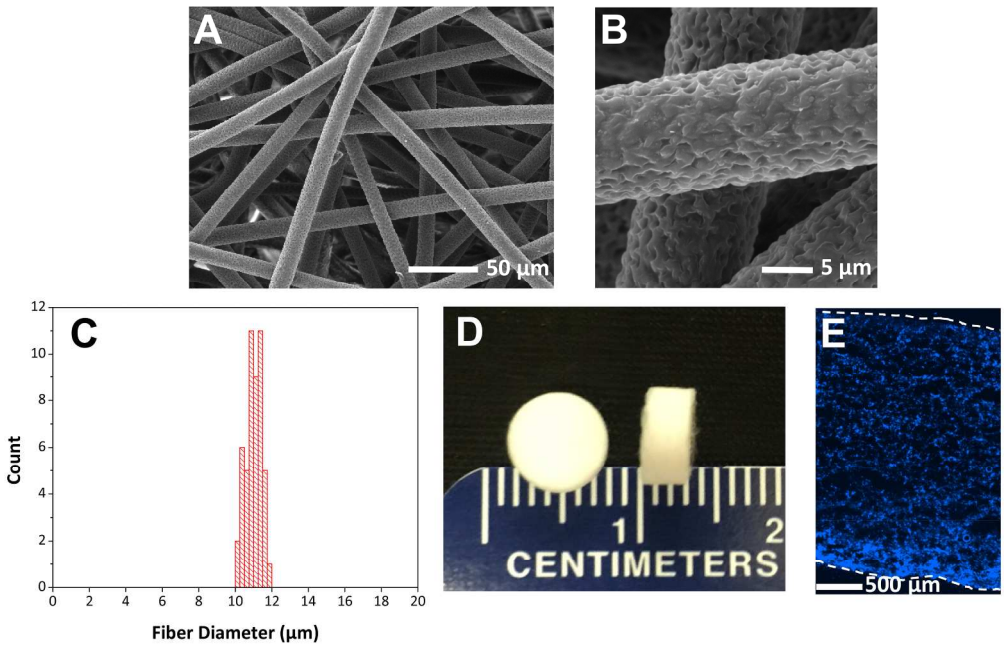

Figure 1. Morphological characterization of electrospun scaffolds. Representative SEM images showing (A) the microstructure of the fibrous network of fibers having (B) the porous surface morphology and (C) a relatively uniform fiber size distribution (n=50). (D) A representative optical image showing the gross morphology and shape of the scaffolds for cell culture as well as (E) a DAPI stained image of a scaffold cross-section depicting complete cellular infiltration throughout the scaffold.

114x74mm (600 x 600 DPI)

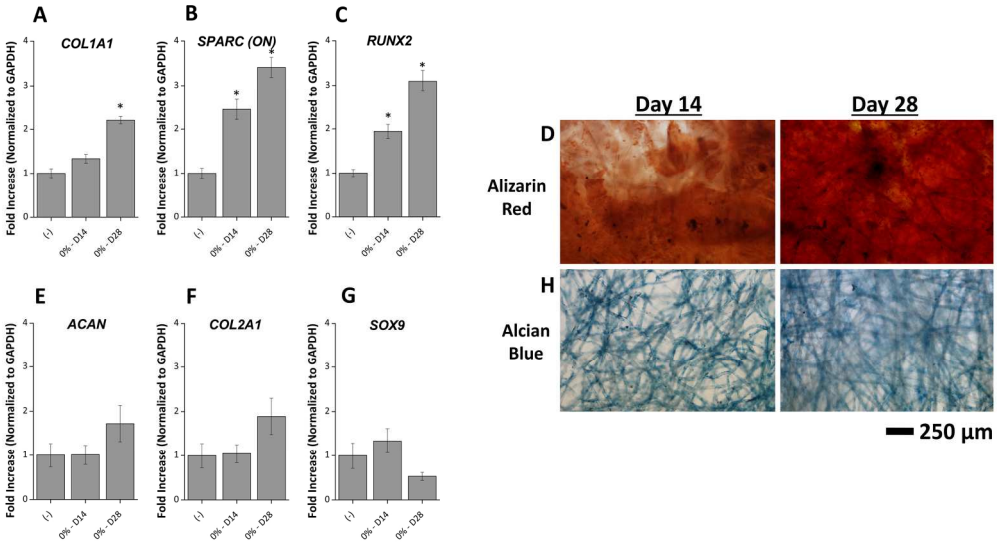

Figure 2. The osteogenic or chondrogenic differentiation of hMSCs cultured in 3D electrospun scaffolds for various durations. (A-C) Greater osteogenic gene expression (COL1A1, SPARC (ON), and RUNX2) and (D) ECM deposition (calcium by alizarin red) as compared to (E-G) chondrogenic gene expression (ACAN, COL2A2, and SOX9) and (H) ECM deposition (glycosaminoglycan by alcian blue) indicate preferential differentiation of hMSCs towards osteogenic lineage under static culture conditions.

95x51mm (600 x 600 DPI)

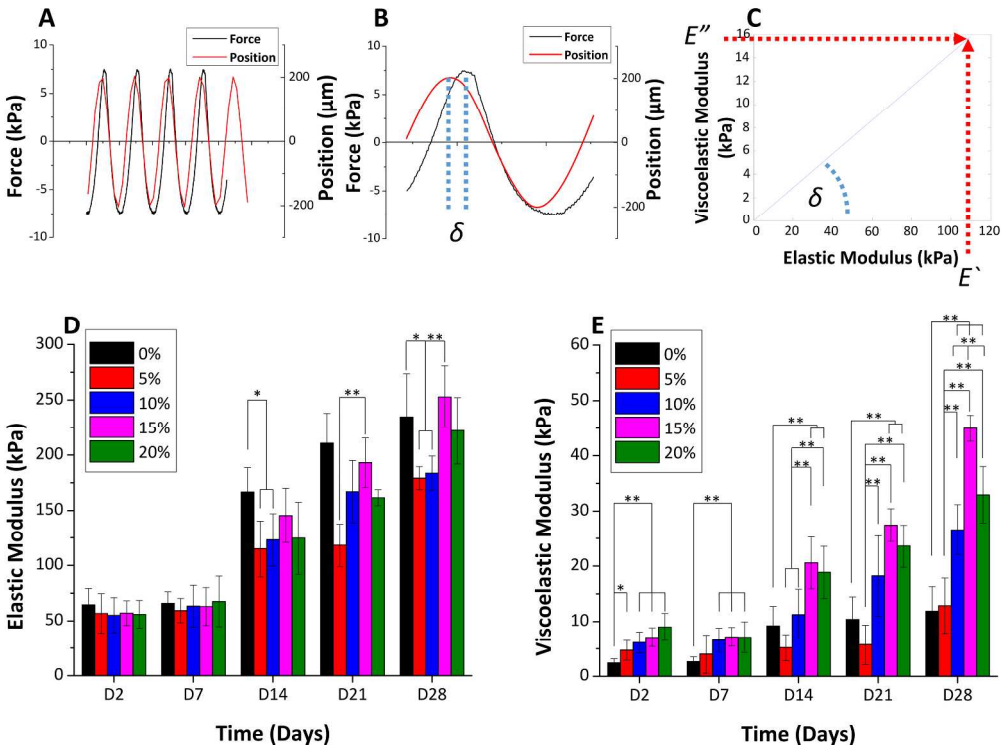

Figure 3. Dynamic mechanical analysis of cell/scaffold constructs cultured under daily mechanical stimulation with various dynamic compressive magnitudes and culture durations. (A) A representative force and position curves acquired from a cell/scaffold construct under sinusoidal dynamic compression, and (B) a detailed force-position curves showing a phase delay (δ) between the applied strain and the responding force, which was used to deconvolute (C) the of elastic (E') and viscoelastic (E") moduli. (D) Deconvoluted elastic and (E) viscoelastic mechanical properties of the cell/scaffold constructs cultured under different magnitudes (5, 10, 15 and 20% strain) of dynamic compression analyzed at different time points up to 28 days. * and ** denote $p < 0.05$ and $p < 0.01$, respectively (n=6).

130x96mm (600 x 600 DPI)

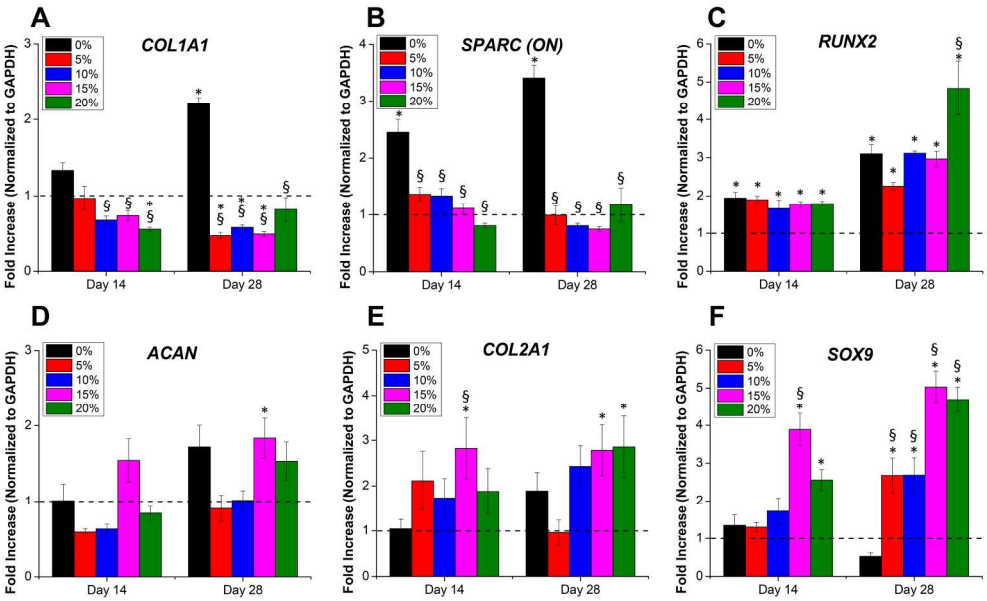

Figure 4. The osteogenic or chondrogenic differentiation of hMSCs by dynamic compressive stimulation with various magnitudes and durations. The relative gene expression of hMSCs dynamically cultured in electrospun scaffolds for up to 28 days determined by qRT-PCR for (A-C) osteogenic markers, COL1A1, SPARC (ON) and RUNX2, and (D-F) chondrogenic markers ACAN, COL2A1 and SOX9. Each gene expression was normalized to that of the cells before being cultured in the scaffold (dashed lines). * and ** denote $p < 0.05$ and $p < 0.01$, respectively, as compared to the negative control samples (represented as dashed lines); § and §§ denote $p < 0.05$ and 0.01, respectively, as compared statically culture samples (0%).

105x63mm (600 x 600 DPI)

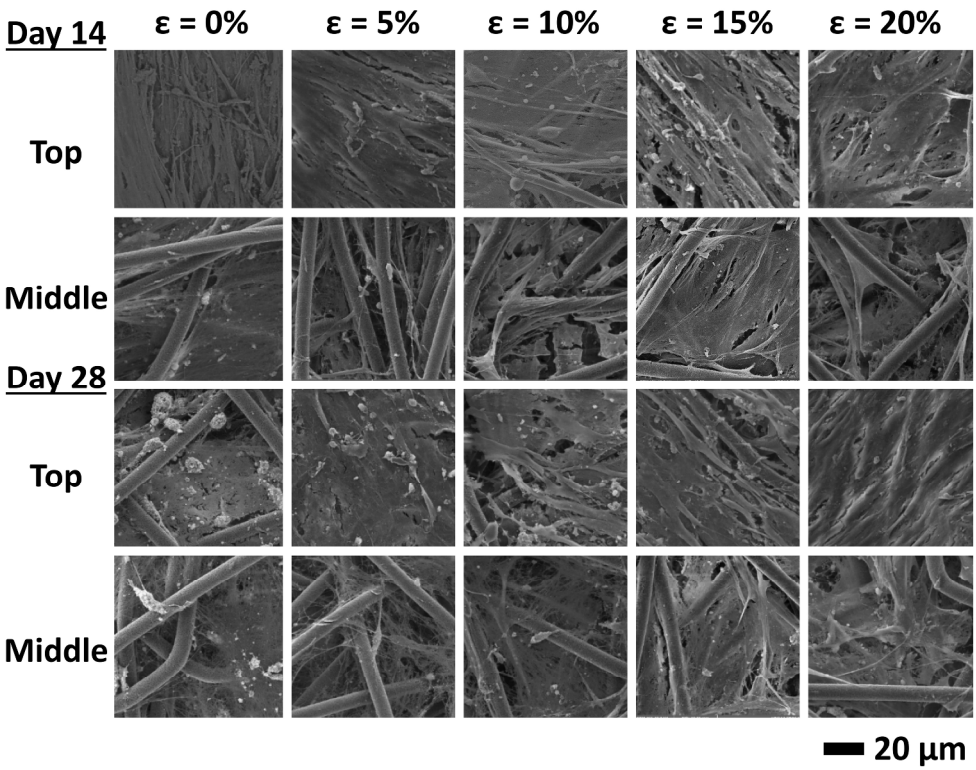

Figure 5. Representative SEM images of cell/scaffold constructs cultured under various conditions. The cell/scaffold constructs cultured under different dynamic compressive stimulation (0, 5, 10, 15 and 20% strain) for 14 or 28 days were subjected to SEM imaging to assess overall ECM deposition.

136x105mm (600 x 600 DPI)

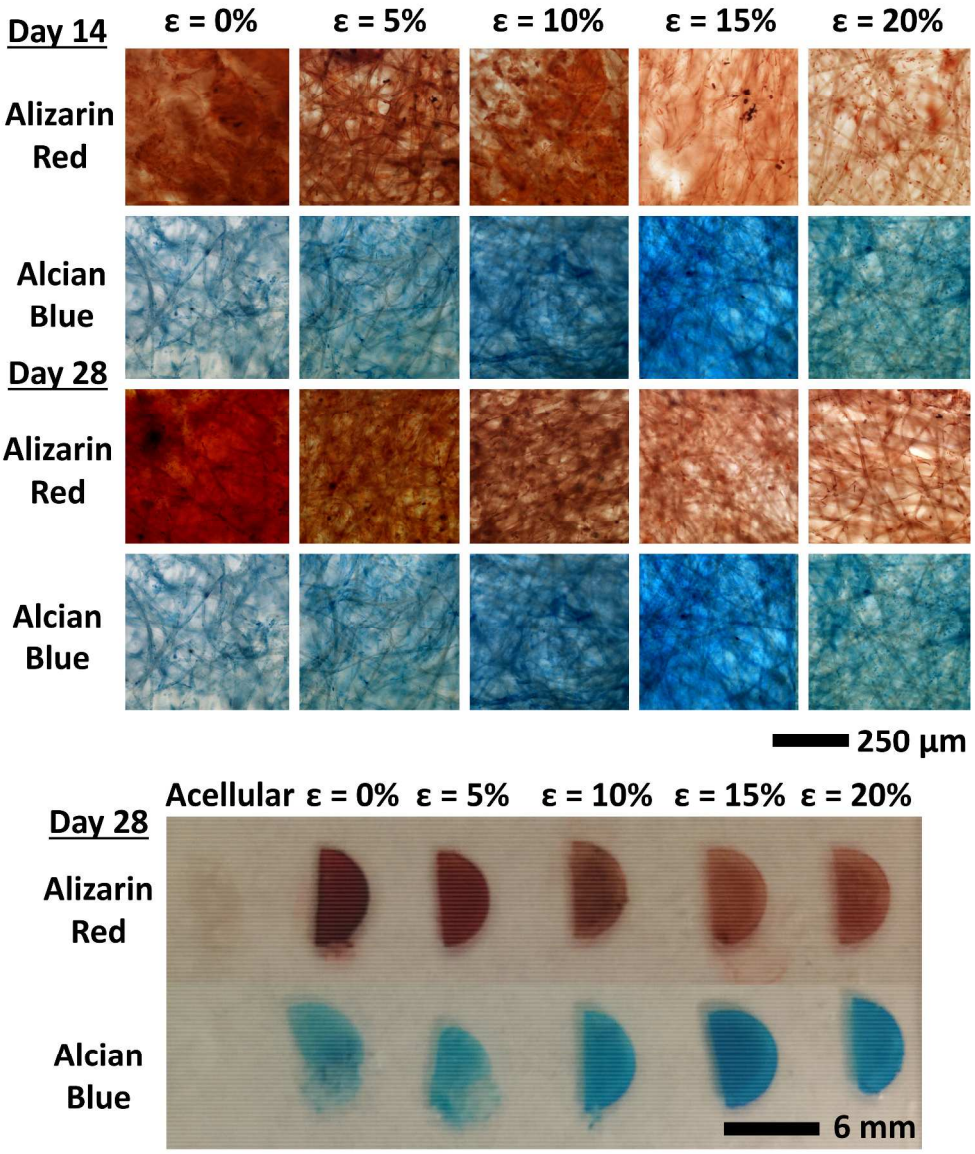

Figure 6. Representative histology images of cell/scaffold constructs cultured under various conditions exhibiting different ECM compositions from hMSCs. The cell/scaffold constructs cultured under different dynamic compressive stimulation (0, 5, 10, 15 and 20% strain) for 14 or 28 days were subjected to histology imaging (alizarin red for calcium and alcian blue for glycosaminoglycan) to assess overall ECM deposition. A macro-scale digital image of scaffold sections at day 28 is also shown.

205x241mm (600 x 600 DPI)

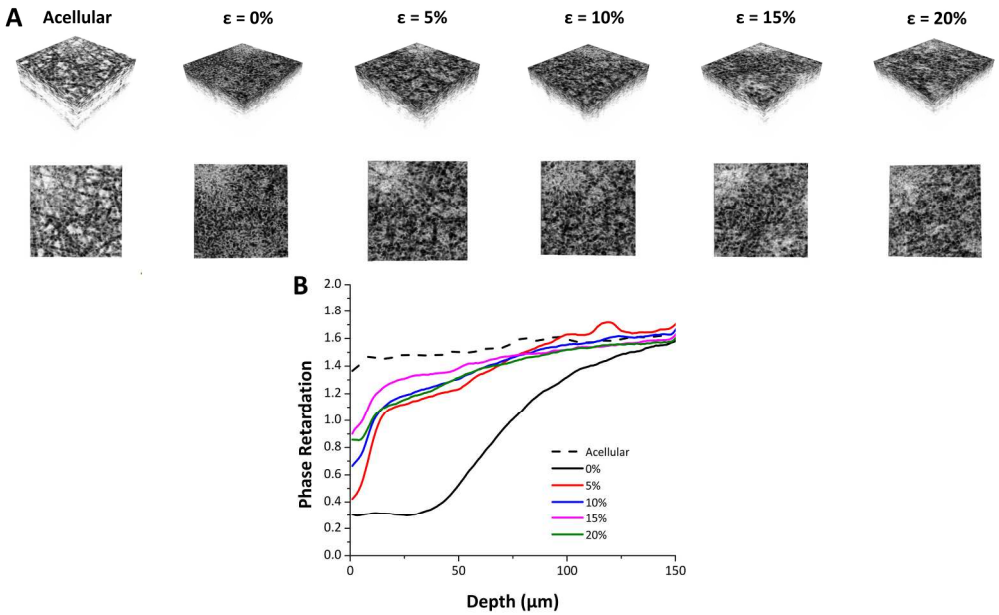

Figure 7. Optical Coherence Tomography (OCT) of acellular and cellular scaffolds cultured with or without dynamic compression. OCT intensity images of (A) acellular scaffold, cell/scaffold constructs cultured (B) without or (C) with dynamic compression, and (D-F) corresponding graphs of double-pass cumulative birefringence from polarization-sensitive OCT analysis.

107x65mm (600 x 600 DPI)